# Real-Time Video Streaming in Multi-hop Wireless Static Ad Hoc Networks


## ABSTRACT

In this paper we deal with the problem of streaming multiple video streams between pairs of nodes in a multi-hop wireless ad hoc network. The nodes are positioned on a plane, know their locations, and are synchronized (via GPS). We consider a 802.11g WiFi network in which NICs can hop between non-overlapping frequency channels in a synchronous fashion. Our goal is to maximize the minimum throughput over all the video streams. We designed a centralized algorithm that computes a channel/time-slot table. Each entry in the table specifies the active links.

Our algorithm constructs a communication graph based on distances. For each link in the communication graph, a set of interfering links is defined based on distances and the SNR of the link. A multicommodity flow with interference constraints is solved by linear programming. The flow is then rounded to obtain the channel/time-slot table. After the table is broadcast, each node receives and transmits according to the table. In addition, we developed a localized flow-control mechanism to stabilize the queue lengths.

We simulated our algorithm using OMNET++/MixiM (i.e., physical SINR interference model) to test whether the computed throughput is achieved. Our results show that we are able to route 70% of the computed throughput.


## 1. INTRODUCTION

We address the problem of routing real-time video streams in static ad hoc wireless networks. Our goal is to develop and implement an efficient algorithm and test it in the realistic physical model.

*Special characteristics of real-time video streaming.*

Streaming of real-time video in a multi-hop ad hoc network is a challenging task. We briefly overview these unique characteristics. (1) End-to-end delay in streaming of real-time video should be as small as possible. We assume that a delay of 1-2 seconds is tolerable if the video has to travel across $10$ hops. One implication of this constraint is that end-to-end acknowledgments and TCP are not an option. (2) Unless erasure codes are employed, loosing even a small fraction of the packets incurs an intolerable degradation in the video quality. We assume that video has acceptable quality if less that $0.5\%$ of the packets are dropped. In wireless networks, each link can have a PER of $1\%$-$5\%$. Thus, after $10$ hops, one is left with intolerable erasures. On the other had, erasure codes incur an extra end-to-end delay since they need to accumulate data for a block before encoding can take place. This means that relying on WiFi acknowledgments and retransmit capabilities can be useful to avoid packet drops if the PER is small. (3) A useful feature in video coding is the ability to adjust the compressed bit-rate. This means that the video encoder can be continuously controlled to generate a video stream of a requested bit rate. We rely on this feature in our flow control algorithm. This feature separates video streaming from other applications such as FTP. The necessity of cross layer designs has been recognized for satisfying the special characteristics of real-time video streaming over wireless networks [Sha05, SYZ$^+$05, KPS$^+$06]. We continue this line of work.

*Previous Work.*

The WiFi technology builds on the 802.11 protocol, where in this paper we used the 802.11g standard. The exact details of the communication, such as RTS/CTS frames, and hold off time are described in detail in [Gas05]. The standard has 8 Modulation Coding Schemes (MCS) that define the data-rate, coding and modulation. The MCSs are ordered from a rate of 6Mbps for MCS $0$ to rate of 54Mbps for MCS 7. The higher the data-rate, the higher the required signal-to-noise ratio (SNR). Adapting the MCS is one of the ways to decrease the error rate in case of change in the SNR [KM97, HVB01].

The multi-hop routing problem for ad hoc networks was investigated thoroughly. While our emphasis is on supporting video streams (i.e., throughout and low end-to-end delay), the main of research focuses on distributed algorithms for packet routing in the case of mobile nodes [JM96, BMJ$^+$98, PR02].

One of the commonly used heuristics for routing is based on finding paths with maximum bottleneck, namely, paths for which the edge with the lowest capacity is maximum [DPZ04]. In [DPZ04], the goal function is a combination of maximizing the bottleneck and the total throughput. We used this algorithm in our benchmarks (we call it SHORTP). A different approach for the routing problem is based on

solving a linear program. In [JPPQ05] Jain et al. used the graph based protocol interference model to approximate the physical SINR-interference model. The protocol model is an approximation to the physical SINR-interference model, since interference from links may accumulate and create an interference. In [JPPQ05], an linear program (LP) is formulated for the problem of routing multiple streams. The LP uses constraints that are based on independent sets in a conflict graph. This method is not polynomial time. Simulations in [JPPQ05] were run with nodes on a grid, however, these simulations are not in the physical model. Following [JPPQ05], Alicherry et al [ABL05] formulated a linear program that can be computed in polynomial time. They simulated their algorithm on a grid and on random scenarios. A similar LP was formulated also in [BSTZ07]. Wan [Wan09] pointed out various errors in previous algorithms and presented a new linear program that corrects the problem. He proved that: (i) there is a 23-approximation algorithm based on the linear program, and (ii) there is a polynomial time scheme (PTAS) for the problem, however, this PTAS is not practical. The linear program presented in [Wan09] is more complicated than the LP in [ABL05, BSTZ07] and is harder to solve. It is not clear if Wan's method is efficient enough to work even with moderate sized networks.

*Our Contributions.*

1. To evaluate our algorithm we perform a simulation of real-time video streaming in a standard 802.11g setting using OMNET++/MixiM (Sec. **??**). In this setting, all WiFi frames are transmitted (i.e., RTS,CTS, packet, ACK), and interferences between frames are analyzed using the SINR and the MCS.

2. We introduce a new interference model that is an intermediate model between the physical SINR-model and the graph based protocol model (Sec. **??**). The interference set of a link is a function of the signal-to-noise ratio of the link and the MCS of the link. As the link is closer to the SINR-threshold, the interference set grows, so that SINR is not in the "waterfall" region of the PER function. One advantage of this new interference model is that it is easy to formulate interference constraints in the linear program formulation (Sec. **??**).

3. We formulate the problem of minimizing end-to-end delay due to a schedule that supports a given multi-flow. We developed and implemented a scheduler algorithm that address this problem of reducing end-to-end delays while supporting a similar throughput. (Sec **??**).

4. We developed and implemented a flow control algorithm that stabilizes the queue lengths and controls the data-rate along the links. This flow control algorithm is executed locally by the nodes.

5. We combine the various aspects of video streaming to analyze performance that is crucial for real-time video streaming. Namely, we measured the throughput, end-to-end delay, fraction of dropped packets, and the stability of these parameters.

## 2. PROBLEM DEFINITION

*Setting.*

We consider a WiFi 802.11g static ad hoc network with 3 non-interfering radio channels with the assumptions: (i) Single radio: each node has a single wireless network interface controller (WNIC). (ii) Each node is equipped with a GPS so that it knows its location and the nodes are synchronized. (iii) The WNICs support quick synchronized hops between frequency channels. (iv) Isotropic antennas. (v) We also assume that the nodes have already joined the network and that there is at least one node (i.e., center node) that holds full information about the network (i.e., nodes and locations). Accumulating this information can be done in a distributed low-bandwidth fashion after building a spanning tree [Awe87].

*Problem Definition.*

The input to the algorithms consists of:

1. A set $V$ of $n$ nodes in the plane. A transceiver is located in each node.

2. A set of $k$ video stream requests $\{r_i\}_{i=1}^{k}$. Each stream request is a triple $r_i \triangleq (a_i, b_i, d_i^*)$, where $a_i$ is the source (e.g., camera) of the stream, $b_i$ is the destination, and $d_i^*$ is the required data-rate.

Ideally, we would like to satisfy all the requests, namely, for each video stream $r_i$, route packets using multi-hops from $a_i$ to $b_i$. We assume that there is there is a path in the network between each source-destination pair.

Let $d_i$ denote the data-rate achieved for the $i$th stream. The service ratio $\rho_i$ of the $i$th demand is defined by $\rho_i \triangleq d_i/d_i^*$. Our goal is to maximize the minimum service ratio, namely, $\max \min_i \rho_i$.

Additional performance measures are: (i) End-to-end delay - this is the time it takes a packet to reach its destination. We are interested in reducing the maximum delay (among the packets that are delivered) since the video is real-time. In addition, the maximum delay determines the size of the jitter buffer in the receiving side. (ii) Number of dropped packets. Queue management may drop packets that never reach their destination. (iii) Queue lengths in intermediate nodes tell us how much memory should be allocated and also give an indication of the delay per hop.

## 3. PRELIMINARIES

### 3.1 Interference Models

*Bidirectional interference.*

The delivery of a message in the WiFi MAC requires transmission of frames by both sides (e.g., RTS and packet are transmitted by the sender, CTS and ACK are transmitted by the receiver). Hence, interferences can be caused also by frames transmitted by a the receiving side.
We outline the three interference models below.

*The SINR model.*

The SINR model, also called the physical interference model, defines successful communication as follows. Let $d_{u,v}$ denote the distance between nodes $u$ and $v$. Suppose a subset $S_t \subseteq V$ of the nodes are transmitting simultaneously in the same frequency channel as $u$. The signal-to-interference-plus-noise ratio (SINR) for the reception by $v \in V \setminus S_t$ of the signal transmitted by $u \in S_t$ in the presence of the transmitters $S_t$ is defined by

$$\text{SINR}(u, v, S_t) \triangleq \frac{P/d_{u,v}^{\alpha}}{N + \sum_{x \in S_t \setminus u} P/d_{x,v}^{\alpha}}.$$

Each transmitter can use one of several modulation coding schemes (MCS). The message transmitted by $u$ in an MCS $m$ is successfully received by $v$ if $\text{SINR}(u, v, S_t) \geq \beta_m$, where $\beta_m$ is the minimum SINR-threshold for the MCS $m$.

*Protocol model.*

The protocol model, also called the graph model, is specified by two radii: (i) A communication distance $r$. (ii) An interference distance $R$. The rule for successful communication between two nodes $u$ and $v$ is that $v$ receives the message from $u$ if $d_{u,v} < r$ and every node $x$ that transmits at the same time satisfies $d_{xv} > R$. In this model, a communication graph is defined over the nodes. Two nodes are linked by an edge if their distance is less than the communication distance $r$.

Since the WiFi MAC requires transmission by both sides, an *interference* is defined between two links $(u, v)$ and $(u', v')$ if $\min\{d_{u,u'}, d_{u,v'}, d_{v,u'}, d_{v,v'}\} < R$. We say that a subset $L$ of links is *non-interfering* if no two links in $L$ interfere. In the protocol model, a *schedule* is a sequence $\{L_i\}_i$ of subsets of non-interfering links.

*The new model.*

The new model is an intermediate model between the SINR model and the protocol model. The idea is that, as the SNR of a link grows, the link can tolerate more interference. Hence, the interference distance is not fixed.

Consider a pair $(u, v)$ of nodes and an MCS $m$. The triple $(u, v, m)$ is a *link* in the new model if $\text{SINR}(u, v, \emptyset) \geq \beta_m$.

Since both sides of a link transmit and receive, the interference set of a link must take into account interferences caused by other transmissions both in the receiver and the sender. However, the frames sent by the receiving side are in MCS 0, therefore, reception of these frames depends on the SINR-threshold $\beta_0$.

The interference set $V_{u,v,m}$ of the link $e = (u, v, m)$ is defined by

$$V_{u,v,m} \triangleq \{x \in V \setminus \{u\} \mid \text{SINR}(u, v, \{x\}) \geq \mu \cdot \beta_i \text{ or } \text{SINR}(v, u, \{x\}) \geq \mu \cdot \beta_0\}.$$

The motivation for this definition is that transmissions of nodes in $V_{u,v,m}$ interfere with the reception of $v$ by $u$, or vice versa. The choice of $\mu = 1.585$ gives us a margin of 2dB above the SINR-threshold. This margin keeps the SINR above the threshold due to interferences caused by transmitters not in $S_{u,v,m}$.

We also define the interfering set of edges with respect to the link $e = (u, v, m)$.

$$I_{u,v,m} \triangleq \{e' = (u', v', m') \mid \{u', v'\} \cap (V_{u,v,m} \cup V_{v,u,m}) \neq \emptyset\} \setminus \{(u, v, m)\}.$$

The interference set $I_{u,v,m}$ contains a link $e'$ if either endpoint of $e'$ interferes with reception at the endpoints $u$ or $v$.

## 3.2 Notation

Let $u$ and $v$ denote nodes and $m$ denote an MCS. A link is a triple $(u, v, m)$ such that $\text{SINR}(u, v, \emptyset) \geq \beta_m$. This definition implies that there can be multiple parallel links between $u$ and $v$, each with a different MCS.

We denote the set of links by $E$. The set $E_{out}(v)$ (resp. $E_{in}(v)$) denotes the set of links that emanate from (resp. enter) $v$. Let $E(v)$ denote the set of links $E_{in}(v) \cup E_{out}(v)$.

For a link $e = (u, v, m)$, let $\text{MCS}(e) = m$, i.e., the MCS $m$ of the link $e$.

# 4. ALGORITHM

## 4.1 Networks Governed by Time-Slotted Frequency Tables

Two tables govern the communication in the network. The first table $A$ is a time-slotted frequency table. The dimensions of $A$ are $F \times T$, where $F$ denotes the number of frequency channels and $T$ denotes the number of time slots. There is one row for each frequency channel and one column for each time slot. (In our implementation we used $F = 3$ and $T = 200$). The table $A$ determines a periodic schedule. The second table is a multi-flow table *mf*. The dimensions of *mf* are $|E| \times [1..k]$ (recall that $k$ equals the number of video streams). The entry $mf(e, s)$ specifies the number of packets-per-period that should be delivered along link $e$ for stream $s$.

Each table entry $A[j, t]$ is a subset of links, i.e., $A[j, t] \subseteq E$. The table governs communication in the sense that, in slot $t'$, the links in $A[j, t' \pmod T]$ try to deliver packets using frequency channel $j$.

We use $A[\cdot, t]$ to denote the set of links $\cup_{j \in F} A[j, t]$. Since we assume that each node is equipped is a single radio, it follows that two links that share an endpoint cannot be active in the same time slot. Hence, for every node $v$, $E(v) \cap A[\cdot, t]$ may contain at most one link.

Algorithm MF-I-S computes a time-slotted frequency table that supports a multi-flow (see Sec. 4.2). A time-slotted frequency tables schedules active links as listed in Algorithm 1. Each node $v$ executes Algorithm TX-RX$(v)$ locally. Since $E(v) \cap A[\cdot, t]$ may contain at most one link, a node $v$ is either a receiver, a sender, or inactive in each time slot. We elaborate below how a queue $Q(v, s)$ with the highest priority for transmission along link $e$ in line 2 in the Transmit procedure is defined.

Upon invocation of Transmit$(e, j)$, where $e = (v, u, m)$, the node $v$ needs to decide which packet to transmit. The node $v$ uses the multi-flow table *mf* to determine the set $S_e$ of streams that are routed along $e$. Since delay is a major issue, it is reasonable to use an EDD-like policy, i.e., pick the oldest packet in the queues $Q(v, s)$, for $s \in S_e$. However, such a policy ignores the remaining number of hops a packet needs to traverse. We prefer the approach that emphasizes fairness. That is, assign a priority that equals the ratio of the number of packets of stream $s$ transmitted along $e$ in the last period divided by the required number. The lower this ratio, the higher priority of the stream. This approach also combines well with the flow control algorithm described in Sec. 5.

## 4.2 Algorithm Specification

*Input.*

The input to Algorithm MF-I-S consists of the following:

1. A set $V \subseteq \mathbb{R}^2$ of nodes in the plane.
2. A set of $k$ video stream requests $\{r_i\}_{i=1}^{k}$. Each request $r_i$ is a triple $r_i \triangleq (a_i, b_i, d_i^*)$, where $a_i$ is the source (e.g., camera) of the stream, $b_i$ is the destination, and $d_i^*$ is the required data-rate.

*Output.*

The output of Algorithm MF-I-S consists of two parts: (i) a time-slotted frequency table $A$, and (ii) a multi-flow *mf*$(e, s)$, for every link $e$ and stream $1 \leq s \leq k$. We note that the units of flow are packets-per-period, where the period is the duration of a time slot times the number $T$ of time-slots in a period.

The multi-flow *mf*$(e, s)$ determines the routing and the throughout of each stream. The role of the frequency/time-slot table $A$ is to specify a periodic schedule that determines which links are active in which time slots.

Although we use fixed length packets (e.g., 2KB), the MCS of a link determines the amount of time required for completing the delivery of a packet. This means, that within one time slot, multiple packets may be delivered along a single link. Let *pps*$(e)$ denote the number of packets-per-slot that can be delivered along $e$. Namely, node $u$ can transmit at most *pps*$(e)$ packets to node $v$ along link $e = (u, v, m)$ in one time-slot. Note that the value of *pps*$(e)$ is a function of the MCS of the link $e$.

**Algorithm 1** TX-RX$(v)$ - a local transmit-receive algorithm for node $v$ as specified by a time-slotted frequency table $A$.

For time slot $t' = 0$ to $\infty$ do

1. $t = t' \pmod T$.
2. if $E_{in}(v) \cap A[\cdot, t] \neq \emptyset$ then {reception mode}
   (a) Let $e \in E_{in}(v) \cap A[\cdot, t]$, where $e(u, v, m) \in A[j, t]$.
   (b) While slot $t$ is not over call Receive$(e, j)$.
3. if $E_{out}(v) \cap A[\cdot, t] \neq \emptyset$ then {transmission mode}
   (a) Let $e \in E_{out}(v) \cap A[\cdot, t]$, where $e(v, u, m) \in A[j, t]$.
   (b) While slot $t$ is not over call Transmit$(e, j)$.

Receive$(e, j)$ - where link $e = (u, v, m)$ and $j$ is a frequency channel.

1. Set tuner to reception in frequency channel $j$.
2. Upon reception of a packet $p$ from stream $s$, insert $p$ to $Q(v, s)$.

Transmit$(e, j)$- where link $e = (v, u, m)$ and $j$ is a frequency channel.

1. Set tuner to transmission in frequency channel $j$.
2. Pick a queue $Q(v, s)$ with a highest priority for transmission along $e$.
3. $p \leftarrow DEQUEUE(Q(v, s))$.
4. Transmit $p$ along $e$.

The table $A$ should satisfy the following properties:

1. Every entry $A[j,t]$ in the table is a set of non-interfering links (in an interference model $\mathcal{I}$). Thus the links in $A[j,t]$ may be active simultaneously.

2. The data-rates $mf(e,s)$ are supported by the table. Namely,

$$\sum_{s=1}^{k} mf(e,s) \leq |\{A[j,t] \mid e \in A[j,t]\}| \cdot pps(e),$$

## 4.3 Algorithm Description

The algorithm consists of two parts: (i) computation of a multi-commodity flow with conflict constraints, and (ii) scheduling of the multi-commodity flow in a time-slotted frequency table. We elaborate on each of these parts.

*Multi-commodity flow with conflict constraints.*

We formulate the problem of routing and scheduling the video streams by a linear program (LP). A similar LP is used in [ABL05, BSTZ07] with respect to the protocol interference model. We use our new interference model for the interference constraints.

For each requested stream $r_i$, we define the supply ratio $\rho_i$ to be the ratio between the flow allocated to the $i$'th stream and the demand $d_i^*$ of the stream. The objective of the LP is to maximize $\min_i \rho_i$. A secondary objective is to maximize the total throughput.

Let $c(e)$ denote the number of packets-per-period that can be delivered along the link $e$ in one period. As in the case of $pps(e)$, the value of $c(e)$ is a function of the MCS of $e$. However, $c(e)$ may be a non-integer, while $pps(e)$ is an integer.

The main variables of the LP are the flow variables $f_i^j(e)$ which signify the amount of flow along link $e$ in frequency channel $j$ for stream $i$. In Eq. 2 we require that the flows are nonnegative. In Eq. 3 we define $f_i(e)$ to be the combined flow along $e$ for stream $i$ over all frequency channels. In Eq. 4 we define $f^j(e)$ to be the combined flow along $e$ in frequency channel $j$ over all $k$ streams. Eq. 5 is simply a flow conservation constraint for stream $i$ in every intermediate node. Eq. 6 is simply a capacity constraint for every link. In Eq 7, the supply ratio $\rho_i$ is defined to be the fraction of the demand for stream $i$ that is supplied. In Eq. 8, $\rho$ is defined to equal the minimum supply ratio, i.e., $\rho = \min_i \rho_i$. Finally, in Eq. 9 the interference constraints are defined; we elaborate on them below.

The objective is to maximize the minimum supply ratio $\rho$. As a secondary objective, we maximize the sum of flows. Therefore, the constant $\lambda$ in the objective function is small (e.g., $\lambda = 1/20$).

The left-hand-side of the interference constraint consists of three addends. The first addend $f^j(e)/c(e)$ is the fraction of the time that the link $e$ is active in transmission in frequency $j$. The second addend is the fraction of time that the endpoints of $e$ are active in transmissions in frequencies less than $j$. Finally, the third addend is the fraction of time in which links in the interference set $I_e$ are active in transmissions in frequency $j$. Recall that each node has a single radio. This implies that the fractions in the last two addends correspond to transmissions that may not take place simultaneously with transmissions in the $j$th frequency channel of link $e$.

We point out that the capacity constraints in Eq. 6 are redundant since they are implied by the interference constraints in Eq. 9.

In our experiments, we noticed that the LP-solver found a solution with flow cycles. We removed these cycles before applying the scheduling step. Interestingly, the issue of flow cycles was not mentioned in previous works [ABL05, BSTZ07]

*Scheduling of the multi-commodity flow in a time-slotted frequency table.*

In the scheduling step we are given the multi-commodity flows $f_i^j(e)$. The task is to allocate entries in a time-slotted frequency table $A$ for these flows.

We first determine how many time-slots should be allocated for $f^j(e)$, for each link $e$ and each frequency channel $j$. Recall that a unit of flow is one packet-per-period. Recall also that $pps(e)$ denotes the number of packets-per-slot that can be delivered along link $e$. This means that the number of time slots in which $e = (u,v,m)$ should be allocated in frequency channel $j$ must be at least

$$|\{t \in [1..T] : e \in A[j,t]\}| \cdot pps(e) \geq f^j(e)$$

Hence,

$$|\{t \in [1..T] : e \in A[j,t]\}| \geq \left\lceil \frac{f^j(e)}{pps(e)} \right\rceil . \qquad (10)$$

*The greedy scheduler.*

The simplest way to assign flows to the table $A$ is by applying a greedy algorithm. The greedy algorithm scans the links and frequency channels, one by one, and assigns $\ell(e,j)$ slots to each link $e$ and frequency channel $j$. Based on [ABL05, KMPS04, BSTZ07], the interference constraints in Eq. 9 imply that the greedy algorithm succeeds in this assignment provided that

$$\ell(e,j) = \left\lfloor \frac{f^j(e)}{pps(e)} \right\rfloor . \qquad (11)$$

The issue of dealing with this rounding problem (i.e., the difference between the round-down and the round-up in Eqs. 10 and 11) is discussed in [Wan09], where it is pointed out that routing all the flow requires a super exponential period $T$. Such a period is obviously not practical; the computation of the table takes too long, the table is too long to be broadcast to all nodes, and the schedule will incur huge delays.

We show that the rounding problem is not an important issue both theoretically and in practice. Since each flow $f_i$ can be decomposed into at most $|E|$ flow paths, it follows that the values of $\{f_i^j(e)\}_{e \in E, j \in F}$ can be "rounded" so that

$$\max \quad \rho + \lambda \cdot \sum_{i=1}^{k} d_i^* \cdot \rho_i \qquad \text{subject to} \tag{1}$$

$$f_i^j(e) \geq 0 \qquad \forall i \in [1..k], \forall j \in [1..3], \forall e \in E \tag{2}$$

$$\sum_{j=1}^{3} f_i^j(e) = f_i(e) \qquad \forall e \in E \tag{3}$$

$$\sum_{i=1}^{k} f_i^j(e) = f^j(e) \qquad \forall e \in E \tag{4}$$

$$\sum_{e \in E_{out}(v)} f_i(e) - \sum_{e \in E_{in}(v)} f_i(e) = 0 \qquad \forall i \in [1..k], \forall v \in V \setminus \{a_i, b_i\} \tag{5}$$

$$\sum_{i=1}^{k} f_i(e) \leq c(e) \qquad \forall e \in E \tag{6}$$

$$\sum_{e \in E_{out}(v)} f_i(a_i) - \sum_{e \in E_{in}(v)} f_i(a_i) = d_i^* \cdot \rho_i \qquad \forall i \in [1..k] \tag{7}$$

$$\rho \leq \rho_i \qquad \forall i \in 1..k] \tag{8}$$

$$\frac{f^j(e)}{c(e)} + \sum_{j' < j} \sum_{e' \in E(u) \cup E(v)} \frac{f^{j'}(e')}{c(e')} + \sum_{e' \in I_e} \frac{f^j(e')}{c(e')} \leq 1 \qquad \forall e = (u, v, m) \in E, \forall j \in [1..3] \tag{9}$$

at most $|E| \cdot \max_e\{pps(e)\}$ packets are lost. Note that this lost flow is bounded by a constant. By increasing the period $T$, the amount of flow tends to infinity, and hence, the lost flow is negligible. In our experiments **??**, we used a period of $T = 200$ time slots, with a duration of $5ms$ per slot. The greedy scheduler was able to schedule almost all the flow in all the instances we considered. The multi-flow table is set so that $mf(e, s)$ equals the amount of flow from $f_s(e)$ that the scheduler successfully assigned.

The greedy scheduler incurred a delay roughly of one period per hop. The reason is that it schedules all the receptions to a node before the transmissions from the node. To avoid this delay, we designed a new scheduler, described below.

*The path-peeling scheduler.*

The path peeling scheduler tries to reduce the time that an incoming packet waits till it is forwarded to the next node. This is achieved as follows.

1. Decomposes each flow $f_i$ into flow paths such that the flow along each path equals the bottleneck, i.e., the minimum $pps(e)$ along the path. Let $\{f_i(p)\}_{p \in \mathcal{P}(i)}$ denote this decomposition.

2. While not all the flow is scheduled,

   (a) For $i = 1$ to $k$ do:

   (b) If $P_i \neq \emptyset$, then schedule $p \in \mathcal{P}(i)$ and remove $p$ from $P_i$.

The scheduling of a flow path $p \in P_i$ tries to schedule the links in $p$ one after the other (cyclically) to reduce the time a packet needs to wait in each node along $p$. The scheduling simply scans the links in $p$ in the order along $p$, and finds the first feasible time slot (in cyclic order) for each link $e \in p$.

We point out that in Line 2a, we schedule one path from each stream to maintain fairness in allocation and delays. On the average, each stream suffers from the same "fragmentation" problems in the table $A$.

In our experiments, the path-peeling scheduler succeeded in scheduling 70% of the flow. The advantage, compare to the greedy scheduler, is that delays are significantly reduced.

## 5. FLOW CONTROL

The multi-flow table computed by the algorithm determines the number of packets $mf(e, s)$ that should be sent along each link $e$ for stream $s$ during each period. Each node $v$ monitors the following information for each link $e \in E_{out}(v)$.

1. $P(e, s, t)$ - the number of packets belonging to stream $s$ sent along the link $e$ during the period $t$.

2. $P^+(e, s, t)$ - the maximum number of packets belonging to stream $s$ that can be sent along the link $e$ during the period $t$. Note that $P^+(e, s, t) \geq P(e, s, t)$; inequality may happen if the queue $Q(e, s)$ is empty when a packet is scheduled to be transmitted along the link $e$. Note that if $e$ is not planned to deliver packets of stream $s$, then $P^+(e, s, t) = 0$.

We remark that a node $v$ can also monitor $P(e, s, t)$ for a link $e \in E_{in}(v)$. However, the value $P^+(e, s, t)$ for a link

$e \in E_{in}(v)$ must be sent to $v$ (e.g., by appending it to one of the delivered packets).

The Flow-Control algorithm is executed locally by all the nodes in the network. Let $e = (u, v, m)$ denote a link from $u$ to $v$, and let $s$ denote a stream. Each node executes a separate instance per stream. In the end of each period $t$, each node $u$ "forwards" the value of $P^+(e, s, t)$ to node $v$. In addition, in the end of each period $t$, node $v$ sends "backwards" the value $R(e, s)$ to $u$. The value $R(e, s)$ specifies the number of packets from stream $s$ that $v$ is willing to receive along the link $e$ in the next period $t + 1$.

The Flow-Control algorithm, listed as Algorithm 2 equalizes the incoming and outgoing packet-rates in intermediate nodes as follows. The requested packet-rate $R(e, s)$ is initialized to be the value $mf(e, s)$ derived from the table. The Flow-Control algorithm is activated in the end of each period. It uses the values $P(e, s, t)$ and $P^+(e, s, t)$ for every link $e$ incident to $v$. Some of these values are computed locally and some sent by the neighbors. The incoming packet-rate $R_{in}$ is computed in line 2c, and is divided among the incoming links in line 2d. Excess packets in the queue $Q(v, s)$ are dropped so that the number of packets in $Q(v, s)$ is at most $R_{in}$. The rational is that, in the next period, at most $R_{in}$ packets will be delivered, and hence, excess packets might as well be dropped.

We now elaborate on the boundary cases of the flow-control for a source $a_s$ and a destination $b_s$ of stream $s$. The destination $b_s$ simply sends an fixed request for each incoming link $e \in E_{in}(b_s)$, i.e., $R(e, s) \leftarrow mf(e, s)$. The source $a_s$, does not execute line 2d; instead, it sets the packet-rate of the video encoder to $R_{in}$.

**Algorithm 2** Flow-Control$(v, s)$ - a local algorithm for managing the local queue and requested incoming rate at node $v$ for stream $s$.

1. Initialize: for all $e \in E_{in}(v)$, $R(e, s) \leftarrow mf(e, s)$.
2. For $t = 1$ to $\infty$ do
   (a) Measure $P(e, s, t)$ for every $e \in E(v)$, and $P^+(e, s, t)$ for every $e \in E_{out}(v)$.
   (b) Receive $P^+(e, s, t)$ for every $e \in E_{in}(v)$, and $R(e, s)$ for every $e \in E_{out}(v)$.
   (c) $R_{in} \leftarrow \min\{\sum_{e \in E_{out}(v)} R(e, s), \sum_{e \in E_{out}(v)} P^+(e, s, t), \sum_{e \in E_{in}(v)} P^+(e, s, t), \}$.
   (d) For every $e \in E_{in}(v)$: $R(e, s) \leftarrow R_{in} \cdot \frac{P^+(e,s,t)}{\sum_{e' \in E_{in}(v)} P^+(e',s,t)}$.
   (e) Drop oldest packets from $Q(v, s)$, if needed, so that $|Q(v, s)| \leq R_{in}$.

# 6. EXPERIMENTAL RESULTS

## 6.1 General Setting

**WiFi parameters.** In the benchmarks that use the scheduler, each node has a single 802.11g WNIC. In the benchmarks that do not use the scheduler, each node has three 802.11g WNICs. The reason is that, in absence of the scheduler, a node does not know to which frequency channel to tune in each moment.

Each WNICs transmits in one of three non-overlapping frequencies. All WNICs transmit at a fixed power ($100mw$). The path loss exponent is $\alpha = 4.1$. The noise figure is $N = -100dBm$. The maximum communication is roughly $150m$ (in MCS 0). An interference $250m$ away, can cause a decrease in the SINR of roughly $1dB$. We used fixed size packets with a payload of $2KB$. Thus, a video stream with a 1Mbps generates $64$ packets per second.

We made the following change in the WNICs when there is a scheduler: The threshold for allowing an RTS frame is reduced to match the interference distance. In this way, communication can be attempted even in times that in the regular setting are not allowed. The justification for this change is that the scheduler takes into account conflicts due to interfering links.

**Software tools.** We used Coin-OR CLP to solve the linear programs. We implemented the scheduler in C++. The simulation was implemented using OMNET++/MixiM. Therefore, the simulation is done in the physical model taking into account path loss, multiple interferences, partial interference between frames, and all the details of the 802.11g protocol.

**Algorithm parameters.** We used $T = 200$ time slots in the time-slotted frequency table. Each time slot has a duration of 5ms.

**Implementation details.** The following simplifications we made in the implementation. (1) Virtual flow control messages are used. They are sent without delay in the end of each period. We justify this simplification since flow control messages are very sparse. (2) Packets of only one stream are sent along each link in each time slot. This simplification only reduces the throughput of the implementation.

## 6.2 Scenarios

We ran the experiments on two main types of arrangements of the nodes in the plane: a circle and a grid.

1. In the grid arrangement, we positioned $49$ nodes in a $1km \times 1km$ square. The nodes are positioned in a $7 \times 7$ lattice, so that the horizontal and vertical distance between adjacent nodes is $1000/7 = 142$ meters (see Fig. 5). The source and destination of the streams in the grid arrangement are chosen randomly.

2. In the circle arrangement, we positioned $24$ nodes on a circle of radius $500$ meters. The nodes were positioned every $360/24$ degrees (see Fig. 6). The source and destination of the streams in the circle arrangement are chosen deterministically, by $a_i = \lceil 24/k \rceil$,

$b_i = (a_i + \lfloor 24/k \rfloor) \bmod 24$, where $k$ denotes the number of streams.

We point out that random locations of $50$ nodes in a square kilometer induces a communication graph with a high degree and a diameter of $2-3$ [MDS10]. In addition, the interference set of each link contains almost the other links. Hence, this setting has a low capacity and is not an interesting setting for the problem we study.

The requests demand $d_i^*$ is set to $50$Mbps. Such a demand with $k \geq 6$ streams is above the capacity of the network. This enables us to study the performance in a congested setting.

## 6.3 Benchmarks

We ran the experiments using five algorithms:

1. SHORTP- a shortest path maximum bottleneck routing algorithm. Let $pps(e)$ denote the number of packets-per-slot in the MCS used by the link $e$. Let $hops(p)$ denote the number of hops along a path $p$. In SHORTP, the stream $s$ is routed along a path $p$ from $a_s$ to $b_s$ such that, for every path $p'$ from $a_s$ to $b_s$, the following holds:

$$\min_{e \in p} pps(e) \geq \min_{e \in p'} pps(e) \text{ , and}$$
$$\min_{e \in p} pps(e) = \min_{e \in p'} pps(e)$$
$$\Longrightarrow hops(p) \leq hops(p').$$

   The paths assigned to the $k$ streams are divided evenly among the three frequency channels.

   Each node in this benchmark contains three radios. This means that each node contains three standard 802.11g WNICs, each working in different frequency channel. Since the frequency channels are non-overlapping, one WNIC may receive while another WNIC is transmitting. Each WNIC receives and transmits packets according to the WiFi MAC. Fairness between the streams is obtained as follows. Each WNIC is given FIFO-queue for each stream, the packets of which it needs to transmit. Each WNIC uses a simple round-robin policy for determining the queue from which the next packet is transmitted.

   The paths are computed in an oblivious manner, namely, congestion does not play a role. This means that we must execute a flow control algorithm to adjust the data-rate. To execute the Flow-Control algorithm without any changes, we trivially cast this routing to our setting as follows. We define the multi-flow $mf(e,s)$ to equal $d_s^*$ if $e$ is in the path assigned to stream $s$, and $0$ otherwise. The time-slotted frequency table $A$ has a single time slot (i.e., $T = 1$) whose duration is one second. Namely, the table $A$ has three entries, one for each frequency channel. The table entry for frequency channel $j$ lists the links that use frequency channel $j$.

2. MF-I-S. In the MF-I-S benchmark all three parts of our algorithm are used: computation of a multicommodity flow with interference constraints, the path-peeling scheduler, and the Flow-Control algorithm,

   We emphasize that in this benchmark, each node contains a single radio; namely, each node has a single standard 802.11g WNIC capable of hopping between the three frequency channels in the beginning of each time slot.

3. MF-S - same as MF-I-S except that the LP does not include interference constraints. The scheduler resolves interferences, so it is interesting to see how much throughput is scheduled by the scheduler, and whether this throughput is routed in the simulation.

   We point out that the interference constraints constitute a large part of the LP constraints. By omitting them, the LP becomes shorter, easier to solves, and naturally, the LP solution has a higher throughput.

   Since the LP lacks interference constraints, the scheduler may fail to schedule the flow. We modified the scheduler in this case so that it augments the table $A$ by adding time-slots. This augmentation has an adverse effect of reducing throughput and increasing delay.

4. MF-I - same as MF-I-S but without the scheduler. Instead, the multi-flows are assigned in a single-slot schedule, as in Algorithm SHORTP. We point out that in this benchmark, each node is equipped with three WNICs as in Algorithm SHORTP.

   The motivation for this benchmark is that the multi-flow takes into account congestion and interference. Since the WiFi MAC deals with avoiding collisions, so it is interesting to see how it succeeds in scheduling the multi-flows in a distributed manner.

   As in SHORTP, each node has three WNICS in this benchmark.

5. MF - similar SHORTP except that the the streams are routed according to a multi-commodity flow. The multi-commodity flow is computed by an LP without interference constraints. This benchmark helps understand whether non-oblivious congestion aware routing improves performance.

   As in SHORTP, each node has three WNICS in this benchmark.

## 6.4 Results

*Routing results.*

The routing result for $k = 12$ streams is depicted for the grid scenario in Fig. 5 and for the circle scenario in Fig. 6. Note that a request may be routed along multiple paths.

| k | MF-I-S's min Throughput | SHORTP's min Throughput | Ratio |
|---|---|---|---|
| | Mbps | Mbps | |
| 8 | 0.448 | 0.368 | 1.217 |
| 12 | 0.336 | 0.24 | 1.4 |
| 16 | 0.144 | 0.112 | 1.285 |

Table 1: The leftmost column lists the number of requests $k$ in the grid scenario. The second row lists the minimum throughout for $k \in \{8, 12, 16\}$ in the MF-I-Salgorithm. The demand for each stream request is 50 Mbps. The third row lists the minimum throughout for $k \in \{8, 12, 16\}$ in the SHORTP. Every entry in the rightmost row corresponds to the ratio between the minimum throughput of MF-I-S and SHORTP.

*Benchmark comparison.*

In Tables 2 and 3 we summarize the measured performance of the benchmarks for the grid and circle scenarios with $k = 12$ requests and a demand $d_i^* = 50$Mbps for each stream. Notice that the MF-I-S and MF-S benchmarks use only one WNIC per node, while the other benchmarks use three WNICs per node.

We begin by discussing the grid scenario: (1) The minimum throughput obtained by MF-I-S is the highest. (2) The sum of the throughputs obtained by SHORTP is 20% higher than that of MF-I-S. (3) The maximum end-to-end-delay obtained by MF-I-S is by far better than the other benchmarks (4) MF-I-Suses longer paths to avoid congestion and interference. (5) The scheduled benchmarks (i.e., MF-I-S and MF-S) have a very small drop rate. (6) All benchmarks have reasonable PER.

In the circle scenario we obtained the following results: (1) The minimum throughput obtained by MF-I-S is 0.35 that of SHORTP. (2) The sum of the throughputs obtained by SHORTP is only twice that of MF-I-S. (3) The maximum end-to-end-delay obtained by MF-I-S is by far better than the other benchmarks (4) MF-I-Suses longer paths to avoid congestion and interference, and utilize all three frequencies. (5) Drop rate are small also for SHORTP. (6) PER is not a problem for MF-I-S, SHORTP, and MF-S.

In light of the fact that MF-I-Suses a single WNIC per node, it is clear that it outperforms all other algorithms. Most importantly, the end-to-end delay in MF-I-Sis much shorter.

*Effect of number of streams.*

Table 1 depicts the effect of the number of requests,$k$, on the minimum throughputs of MF-I-S and SHORTP in the grid scenario. The number of requests $k$ is $8, 12, 16$. The demand for every stream request is 50 Mbps.

Clearly, the min-throughput decreases as the number of requests increases, as the same resources need to serve more requests. The advantage of MF-I-S is maintained for this range of requests.

*Effect of single radio on* SHORTP.

Since SHORTP uses 3 WNICs per node, we experimented also with a single WNIC per node. Figure 1 depicts the effect of single radio on total throughput of SHORTP. The ratio is almost constant and equals 3, as expected.

The experiment was made in the grid arrangement, where The number of requests is $k = 12$. The demand for every stream request is 50 Mbps.

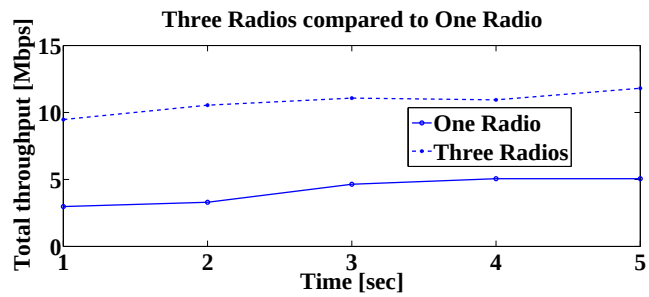


Figure 1: Comparison of total throughput for SHORTPin the grid scenario with $k = 12$ and $d_i^* = 50$Mbps.

*Fairness.*

Figure 2 compares the sorted throughputs achieved for the streams in MF-I-S and SHORTP. The experiment was made in the grid arrangement, with $k = 16$ streams and $d_i^* = 50$ Mbps.

Although SHORTP has a higher total throughput, the 7 with the smallest throughputs have less throughput in SHORTPthan in MF-I-S. This means that SHORTPfavors short links, and is less fair than MF-I-S.

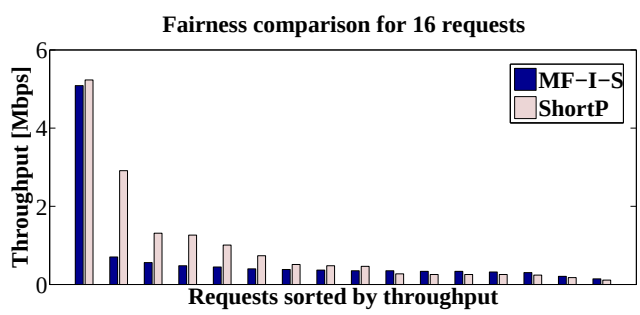


(a)

Figure 2: Streams in each benchmark are sorted by their throughput for the grid arrangement with $k = 12$.

*The Flow-Control algorithm.*

Figure 3 depicts the effects of the Flow-Control algorithm in the grid arrangement with $k = 12$ and $d_i^* = 50$Mbps. In Fig. 3a, the requested rates $R(e, s)$ are depicted. It can be seen that only slight perturbations occur over time. This justifies our simplified implementation that uses virtual flow-control messages.

In Fig. 3b, the queue lengths of the stream in three different nodes are depicted. The oscillation is due to the periodic

schedule. The queue length is controlled and stabilizes.

In Fig. 3c, the drop ratio is depicted for the worst stream. The drop rate ranges from 0 to 1.5%.

In Fig. 3d, the differences between the maximum and minimum throughput for MF-I-S and SHORTP are depicted for all streams two seconds after the beginning of the experiment. It is evident that MF-I-S is more stable than SHORTP since the differences are smaller.

*Comparison with greedy scheduler.*

In Figure 6.4 we compare MF-I-S with the greedy scheduler and the path-peeling scheduler. The throughput obtained with the path-peeling scheduler is smaller, the end-to-end delay is significantly improved.

## 7. CONCLUSIONS

In terms of the stream with the minimum throughput, MF-I-S outperforms the SHORTP algorithm with a single WNIC. In the grid, MF-I-S even outperforms SHORTP with 3 WNICS per node. We attribute this to the routing that may use multiple paths per stream.

In terms of end-to-end delay, MF-I-S outperforms all the benchmarks even when it uses paths that are much longer.

The average drop rate for MF-I-S is below 0.2%. This makes the algorithm feasible for reliable communication of real-time video streams.

We summarize our conclusions by noting that the performance of MF-I-S is stable and predictable, and competes well with nodes equipped with 3 radios in the SHORTP benchmark.

## 8. DISCUSSION

We propose a centralized algorithm for computing a routing, scheduling, and frequency assignment for real-time video streams in static ad hoc wireless networks. The algorithm consists of two parts: a linear program and a scheduler. In addition, each node locally runs a flow-control algorithm to control the queues and stabilize data-rate along the links. Although the algorithm is centralized, it can be executed by multiple nodes in the network provided that they hold full information of the network (i.e., locations, requests). The output of the algorithm consists two tables that easily be broadcast to all the nodes.

We implemented the algorithm and experimented using a setting that uses the physical model to verify the validity of the algorithm. Our experiments show that the algorithm performs well in two congested scenarios.

Future work should address methods for approximate distributed algorithms for solving the linear program and for scheduling. In addition, it is interesting to study the performance of the algorithm when users are mobile. It may be the case that performance does not degrade quickly, so that new tables can be recalculated continuously.

## 9. REFERENCES

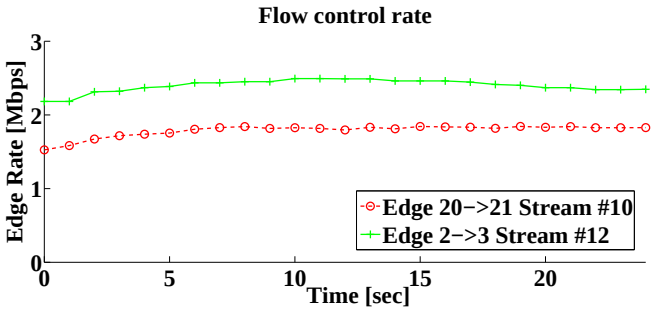


(a) Change in the requested packet rate by the flow-control over time

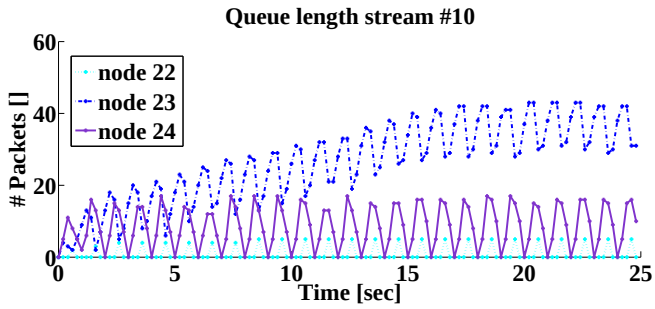


(b) Queue lengths of a stream in three different nodes

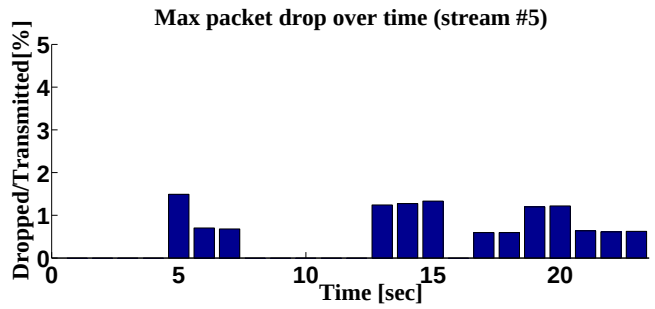


(c) Ratio of dropped packets to transmitted packets over time in worst stream

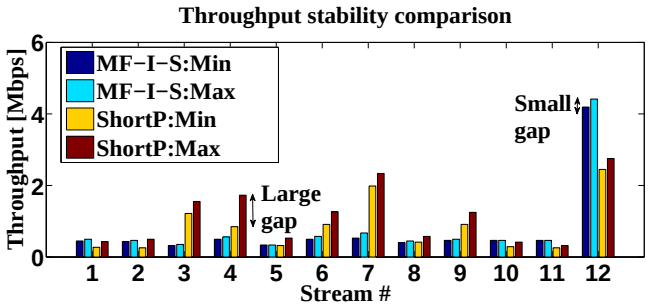


(d) Comparison of stability of throughput between MF-I-S and SHORTP

Figure 3: Influence of the Flow-Control algorithm in the grid arrangement with $k = 12$

[ABL05] M. Alicherry, R. Bhatia, and L.E. Li. Joint channel assignment and routing for throughput optimization in multi-radio wireless mesh

| | #radios | throughput | | | Delay | delay based on hops | | | | hops | drops | PER |
|---|---|---|---|---|---|---|---|---|---|---|---|---|
| | per node | min | sum | max | max | max | | min | | avr | max | avr |
| | | Mbps | Mbps | Mbps | sec | #hops | sec | #hops | sec | | % | % |
| MF-I-S | 1 | 0.336 | 9.776 | 4.416 | 2.1 | 13 | 0.78 | 1 | 0.21 | 6.667 | 0.19 | 1.35 |
| SHORTP | 3 | 0.24 | 11.808 | 2.752 | 3.8 | 9 | 3.8 | 1 | 1.35 | 4.5 | 20 | 1.225 |
| MF-I | 3 | 0.016 | 4.064 | 1.456 | 3.8 | 13 | 1.8 | 1 | 1.05 | 6.667 | 21 | 4.53 |
| MF | 3 | 0.064 | 3.232 | 0.96 | 3.8 | 15 | 1.8 | 2 | 1.4 | 7.33 | 20 | 1.35 |
| MF-S | 1 | 0.09 | 2.504 | 0.53 | 15 | 15 | 4.5 | 2 | 4 | 7.33 | 0 | 1.03 |

Table 2: Compariosn of the benchmarks for the grid scenario with $k = 12$ requests and $d_i^* = 50$mbps for each stream

| | #radios | throughput | | | Delay | delay based on hops | | | | hops | drops | PER |
|---|---|---|---|---|---|---|---|---|---|---|---|---|
| | per node | min | sum | max | max | max | | min | | avr | max | avr |
| | | Mbps | Mbps | Mbps | sec | #hops | sec | #hops | sec | | % | % |
| MF-I-S | 1 | 1.616 | 28.24 | 2.688 | 0.47 | 22 | 0.43 | 2 | 0.47 | 3.667 | 0 | 0 |
| SHORTP | 3 | 4.592 | 57.888 | 4.88 | 1.1 | 2 | 1.1 | 2 | 1.1 | 2 | 1 | 0 |
| MF-I | 3 | 0.72 | 14.784 | 1.76 | 1.95 | 22 | 1.9 | 2 | 1.95 | 3.667 | 14 | 3.52 |
| MF | 3 | 0.576 | 14.736 | 1.888 | 2.25 | 22 | 1.9 | 2 | 2.25 | 3.667 | 17 | 4.02 |
| MF-S | 1 | 1.042 | 18.537 | 1.823 | 2.3 | 22 | 0.95 | 2 | 2.3 | 3.667 | 0.9 | 0 |

Table 3: Compariosn of the benchmarks for the circle scenario with $k = 12$ requests and $d_i^* = 50$mbps for each stream


networks. In *Proceedings of the 11th annual international conference on Mobile computing and networking*, pages 58–72. ACM, 2005.

[Awe87] B. Awerbuch. Optimal distributed algorithms for minimum weight spanning tree, counting, leader election, and related problems. In *Proceedings of the nineteenth annual ACM symposium on Theory of computing*, pages 230–240. ACM, 1987.

[BMJ+98] J. Broch, D.A. Maltz, D.B. Johnson, Y.C. Hu, and J. Jetcheva. A performance comparison of multi-hop wireless ad hoc network routing protocols. In *Proceedings of the 4th annual ACM/IEEE international conference on Mobile computing and networking*, pages 85–97. ACM, 1998.

[BSTZ07] C. Buragohain, S. Suri, C. Tóth, and Y. Zhou. Improved throughput bounds for interference-aware routing in wireless networks. *Computing and Combinatorics*, pages 210–221, 2007.

[DPZ04] R. Draves, J. Padhye, and B. Zill. Routing in multi-radio, multi-hop wireless mesh networks. In *Proceedings of the 10th annual international conference on Mobile computing and networking*, pages 114–128. ACM, 2004.

[Gas05] M.S. Gast. *802.11 wireless networks: the definitive guide*. O'Reilly Media, Inc., 2005.

[HVB01] G. Holland, N. Vaidya, and P. Bahl. A rate-adaptive MAC protocol for multi-hop wireless networks. In *Proceedings of the 7th annual international conference on Mobile computing and networking*, pages 236–251. ACM, 2001.

[JM96] D.B. Johnson and D.A. Maltz. Dynamic source routing in ad hoc wireless networks. *Mobile computing*, pages 153–181, 1996.

[JPPQ05] K. Jain, J. Padhye, V.N. Padmanabhan, and L. Qiu. Impact of interference on multi-hop wireless network performance. *Wireless networks*, 11(4):471–487, 2005.

[KM97] A. Kamerman and L. Monteban. WaveLAN®-II: a high-performance wireless LAN for the unlicensed band. *Bell Labs technical journal*, 2(3):118–133, 1997.

[KMPS04] VS Kumar, M.V. Marathe, S. Parthasarathy, and A. Srinivasan. End-to-end packet-scheduling in wireless ad-hoc networks. In *Proceedings of the fifteenth annual ACM-SIAM symposium on Discrete algorithms*, pages 1021–1030. Society for Industrial and Applied Mathematics, 2004.

[KPS+06] S. Khan, Y. Peng, E. Steinbach, M. Sgroi, and W. Kellerer. Application-driven cross-layer optimization for video streaming over wireless networks. *Communications Magazine, IEEE*, 44(1):122–130, 2006.

[MDS10] M.K. Marina, S.R. Das, and A.P. Subramanian. A topology control approach for utilizing multiple channels in multi-radio wireless mesh networks. *Computer Networks*, 54(2):241–256, 2010.

[PR02] C.E. Perkins and E.M. Royer. Ad-hoc on-demand distance vector routing. In *Mobile Computing Systems and Applications, 1999. Proceedings. WMCSA'99. Second IEEE Workshop on*, pages 90–100. IEEE, 2002.

[Sha05] Y. Shan. Cross-layer techniques for adaptive video streaming over wireless networks. *EURASIP journal on applied signal processing*, 2005:220–228, 2005.

[SYZ+05] E. Setton, T. Yoo, X. Zhu, A. Goldsmith, and B. Girod. Cross-layer design of ad hoc

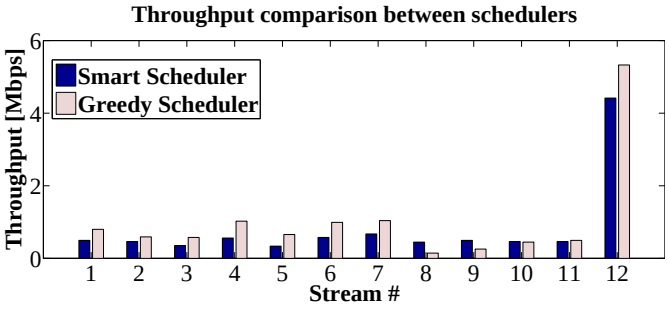


(a) Comparison of throughput

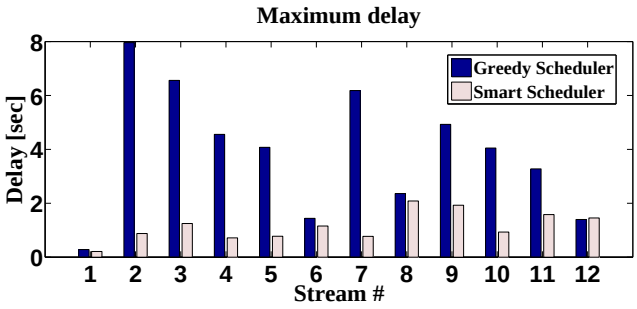


(b) Comparison of end-to-end delay

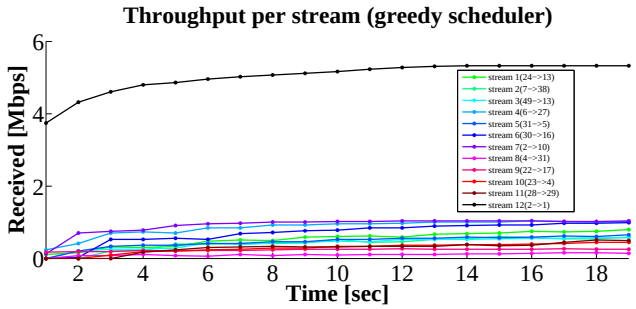


(c)

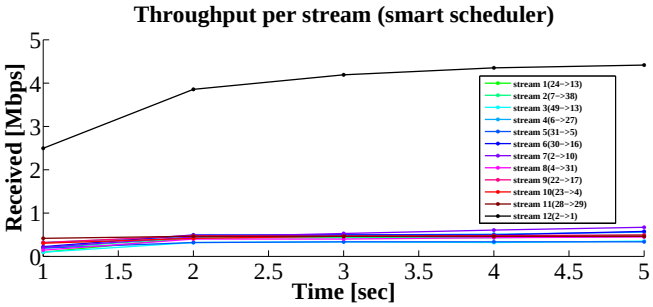


(d)

Figure 4: Comparison of MF-I-S with the greedy scheduler and the path-peeling scheduler

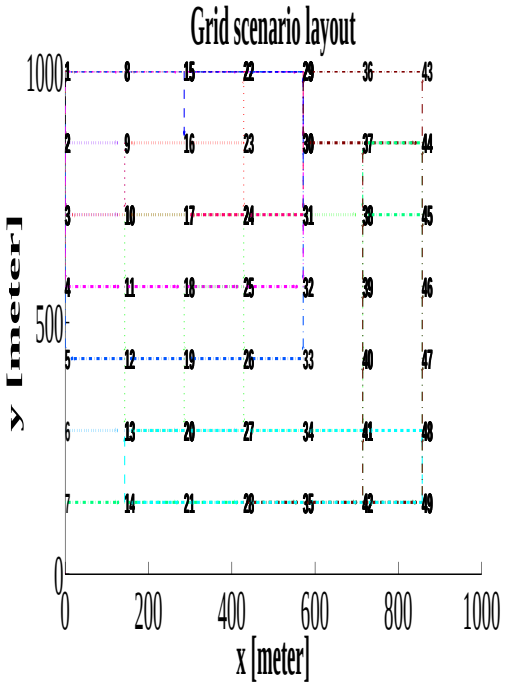


Figure 5: The grid scenario with 49 nodes

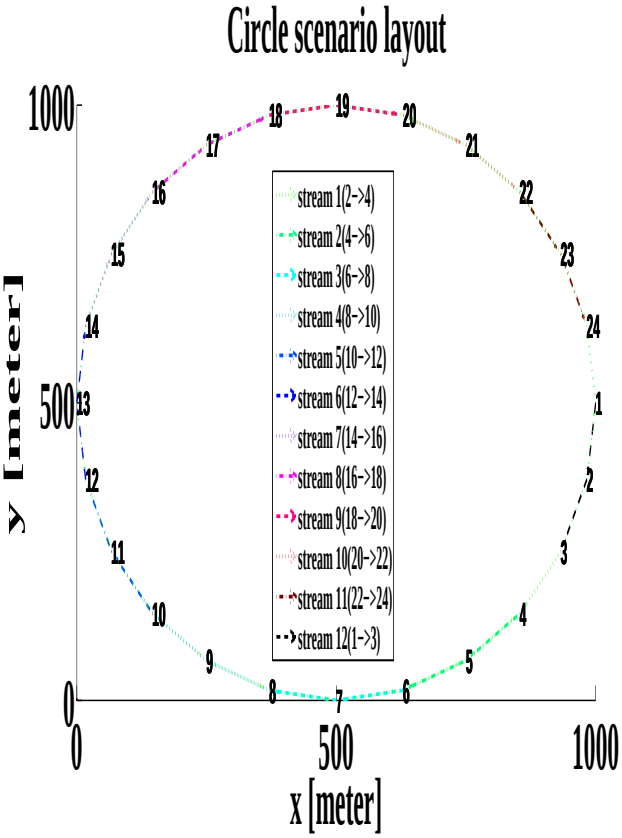


Figure 6: The circle scenario with 24 nodes


networks for real-time video streaming. *Wireless Communications, IEEE*, 12(4):59–65, 2005.

[Wan09] P.J. Wan. Multiflows in multihop wireless networks. In *Proceedings of the tenth ACM*

*international symposium on Mobile ad hoc networking and computing*, pages 85–94. ACM, 2009.